# Theoretical aspects of a.c. deposition of copper and copper oxygenous compounds in alumina pores from Cu(II)-triethanolamine solutions

**Arūnas Jagminas, Vidmantas Kapočius, Ona Nivinskienė, and Svetlana Lichušina**

*Institute of Chemistry, A. Goštauto 9, LT-2600, Vilnius, Lithuania*

The deposition of Cu, $Cu_2O$, CuO, and $Cu(OH)_2$ into a porous alumina template during a.c. electrolysis from acid to alkaline Cu(II) – triethanolamine (TEA) solutions was studied by FTIR spectra and by material balance analysis of all species. The FTIR spectrum of porous alumina after a.c. treatment in weakly acidic Cu(II)–TEA solutions was found to consist of a main peak located at 616 $cm^{-1}$ characteristic of $Cu_2O$ lattice vibrations and two at 421 and 506 $cm^{-1}$ characteristic of $Cu(OH)_2$. The species deposited into the alumina pores from alkaline solutions was found to consist of CuO (sharp and broad modes in FTIR spectrum at 531 and 592 $cm^{-2}$, respectively,), $Cu(OH)_2$ and $Cu_2O$ mixture. The data were verified by equilibrium concentration calculation of all species in the solutions under investigation. From voltammetric studies it was determined that the first process, with increasing the cathodic potential, is hydrogen evolution resulting in an increase of pH at the bottom part of the alumina nanotubes up to $Cu(OH)_2$ formation. A possible mechanism of the formation of copper oxygenous compounds during a.c. treatment in various Cu(II)–TEA solutions is discussed.

**Key words***:* alumina template, copper oxides, triethanolamine solutions, a.c. deposition, FTIR, mass balance

## INTRODUCTION

Copper oxides are widely used as photochemically active, photoconductive and semiconducting compounds [1], as catalysts for the electrooxidation of several classes of organic compounds [2], as sensors [3, 4] or light-to-electricity converters [5]. Additionally, the electronic and photonic characteristics of square $Cu_2O$ layers separated from CuO chains by more or less ionic regions [6] make them fundamental compounds for high-$T_c$ superconductors. Some earlier attempts have been made to synthesize nanometer-size copper oxides uncoated as well as coated with different polymers. CuO particles uniformly coated with polyaniline [7] and polypyrrole [8] have been prepared by metal organic decomposition techniques. Cohen et al. [9] have synthesized copper oxide nanoclusters within the films of diblock copolymers. Xu and co-workers [10] have synthesized CuO nanocrystals by a one-step solid-state reaction, and Goodman et al. [11] on $SiO_2$ by spin coating. Uniformly dispersed copper oxide nanoparticles have been synthesized in poly(vinyl alcohol) by the sonochemical method [12].

The peculiarities of $Cu_2O$ and $Cu(OH)_2$ electrochemical growth on copper surfaces in mildly acidic, neutral, and alkaline solutions have been studied *in situ* in numerous works using FTIR [13, 14], Raman [15–17], SER [18], X-ray photoelectron [19–23], electrochemical impedance [24, 25], ion-scattering [26], and photoacoustic [27] spectroscopy. These studies and electrochemical polarization curves have shown that copper forms a $Cu_2O/CuO,Cu(OH)_2$ douplex film at potentials above 0.78–0.059 pH (*vs.* SHE) in weakly acidic and alkaline solutions [25]. The thickness of the copper anodic films does not exceed 6 nm, except in strongly alkaline solutions. The passive films have a duplex structure represented by an outer $CuO,Cu(OH)_2$ layer overlying the barrier $Cu_2O$. According to Seo et al. [28], the average composition of the outer oxide layer could be represented as $CuO_x(OH)_{2-2x}$, where the value of $x$ varies in the range of x = 0–1, corresponding to the composition range of $Cu(OH)_2$ to CuO. The thermodynamic and kinetic aspects of $Cu_2O$ growth at the

* Corresponding author. Tel.: +370-2 61 17 08. Fax: +370-2 61 70 18. *E-mail address:* jagmin@ktl.mii.lt

Cu/Cu(II)–ethylendiamine interface have been recently analyzed by Survila et al. [29] and showed two regions of $Cu_2O$ stability. One of them is in a slightly acidic and the other one in a strongly alkaline pH region (pH > 12). The formation of thin surface layers of cuprous oxide on the copper surface can be characterized quantitatively by formal electrochemical kinetic equations. However, there is a certain obscurity in the studies of bulk oxide or hydroxide formation in mildly acidic to alkaline pH regions, since the Pourbaix diagrams are of limited use for complex solutions [30].

In order to have a more complete picture of copper oxide/hydroxide formation in the openings of an alumina template during a.c. treatment $Cu(SO_4)$–TEA complex solutions of various acidity were studied in more detail.

## EXPERIMENTAL

### *Materials*

Experiments were carried out using 99.5% grade Al foil containing Fe 0.24, Si 0.2, Cu 0.03, Zn 0.02 and Ti 0.01% (trade mark AD 0, Russia). Specimens of the total surface area 50 $cm^2$ (50 × 50 × 0.075 mm) or 4 $cm^2$ (10 × 20 × 0.075 mm, only for voltammetric measurements) were cut from a rolled sheet. In addition, high-grade Al (99.99%, Goodfellow Cambridge Ltd.) specimens (10 × 20 × 0.125 mm) annealed in vacuum at 773 K for 3 h in order to enhance the grain size in the metal were used for almost ideal structure alumina template formation.

All solutions were prepared from doubly distilled water, high grade acids and chemical grade $CuSO_4 \cdot 5H_2O$ purchased from Aldrich. Before use, triethanolamine was purified by distillation at 473 K under reduced pressure. Other chemicals used in this work were at least of analytical grade.

### *Procedures*

The surface of Al specimens before anodizing was degreased in ethanol, etched in 1.5 M NaOH solution (328–331 K, 30 s), de-smutted in 1.5 M $HNO_3$ solution for 30 s, rinsed and dried. High-grade Al surface was electropolished in a 70/10/20 v/v of $C_2H_5OH$ / glycerol / $HClO_4$(52%) solution (283 K, 12,5 A · $dm^{-2}$, 180 s). The oxide layer from the Al surface was removed by etching for 60 s in 0.24 M $Na_2CO_3$ solution at 353 ± 1 K. Porous alumina templates 2 to 15 ± 0.5 μm thick were grown in a stirred sulphuric acid solution (1.53 M, 291 ± 0.5 K) by applying 15 V from a regulated power supply (0–40 V, 2.5 A, d.c. power supply). In addition, for almost ideal honeycomb porous alumina structure formation, the high-grade Al samples were anodized in vigorously stirred 0.5 M $H_2SO_4$ solution (283 K, d.c. 25 V, 2 h) in accordance with [31]. Two Pb sheets were used in anodizing baths as cathodes. After formation the porous alumina was rinsed with flowing distilled water for 120 s and transferred immediately in the solution for a.c. treatment.

Sine-wave a.c. of industrial frequency 50 Hz was used to deposit copper and copper oxygenous compounds into the alumina template from 0.1 M $CuSO_4$ solution containing 0.02 to 1.2 M TEA and $H_2SO_4$ to adjust the pH of the solutions from 9.5 to 1.5. A.c. electrolysis was carried out at a constant average voltage value ($U_v$) from 6.0 V to 25 V measured by a voltammeter of an electromagnetic system. Seven graphite rods were used as the auxiliary electrodes. All experiments were carried out at ambient temperature.

Voltammetric measurements were carried out in a conventional three-electrode one-compartment water-jacketed glass cell using a PI 50–1.1 potentiostat equipped with a PR-8 programmer and controlled by a PC. A carbon rod was used as the auxiliary electrode. A Cu | $CuSO_4$ (99.999% grade Cu in 0.2 M $CuSO_4$ + 0.5 M $H_2SO_4$, 290 mV *vs.* SHE) electrode was used as the reference electrode connected to the cell via a Luggin capillary whose tip was placed ~1 mm from the electrode surface. The voltammograms were recorded up to –30 V at the potential sweep rate of 0.1 to 1.5 V · $s^{-1}$. Prior to use, the solutions were de-aerated by an argon stream for 0.5 h. All potential values in this paper are referred to the standard hydrogen electrode (SHE).

The colour of alumina was estimated visually.

The phase composition of the colouring species deposited into the pores of alumina template from various Cu(II)–TEA solutions was investigated using the Fourier transform infrared transmission spectra. Porous alumina used in the FTIR studies were sealed in boiling water and separated from aluminium by dissolving it in a solution of 0.65 M bromine in methanol, then rinsed in ethanol, and dried. For recording the compensated FTIR spectra, the powdered porous alumina was dispersed in KBr pellets (4 mg alumina in 500 mg KBr). FTIR spectra were taken on a BOMEM MB (Hartmann and Braun, Canada) spectrometer, which was operated from 800 to 400 $cm^{-1}$ at ambient temperature. Background correction was made using a reference blank KBr pellet pressed with the pure alumina powder (4 mg in 500 mg KBr).

## RESULTS AND DISCUSSION

FTIR spectra have been used for a long time to investigate the composition of cuprous oxide $Cu_2O$

[32–34], cupric oxide CuO [34, 35–41], and cupric hydroxide $Cu(OH)_2$ [33, 42, 43] in the bulk materials and thin surface layers. Factor group analysis using the tables given by Rousseau et al. [44] predicts two IR active modes at 143 and 608 $cm^{-1}$ for cubic $Cu_2O$ lattice [45], six IR active modes at phonon frequencies of 147, 161, 331, 470, 530, and 590 $cm^{-1}$ for a polycrystalline CuO lattice [40, 44, 46] and three IR active modes at 240, 422, and 486 $cm^{-1}$ for $Cu(OH)_2$. The FTIR spectra of porous aluminas, recorded after deposition of about 100 μg $cm^{-2}$ of copper by a.c. treatment in various Cu(II)–TEA solutions at pH 1.5, 4.5, and 8.5 are depicted in Fig. 1. As seen from the presented spectra, the absorption bands at 614, 616, and 621 $cm^{-1}$ for copper species deposited at pH 1.5, 4.5, and 8.5, respectively, are considered to be characteristic of $Cu_2O$. These values are very close to the calculated $Cu_2O$ active mode at 608 $cm^{-1}$ [45] and to that previously reported for $Cu_2O$ films (630 $cm^{-1}$) [33]. In addition, it is apparent that the sharp bands at 421 and 506 $cm^{-1}$ in the obtained spectrum of porous alumina after a.c. treatment in weakly acid solution (Fig. 1b) are close to calculated ones for $Cu(OH)_2$ lattice vibrations at 422 and 486 $cm^{-1}$ and to those previously determined at 418 and 505 $cm^{-1}$ for $Cu(OH)_2$ powder in Nujol mull [33]. In conclusion, the copper deposited in the pores of alumina during a.c. treatment in slightly acid Cu(II)–TEA solutions which colours the template with a greenish tint consists of at least $Cu_2O$ and $Cu(OH)_2$ mixture.

The FTIR spectrum of porous alumina after a.c. treatment in an alkaline Cu(II)–TEA solution is more complicated (Fig. 1c). The assignment of the sharp absorption band in this spectrum at 531 $cm^{-1}$ is indubitably attributed to the Cu–O stretching vibration. Furthermore, the other broad mode with a maximum at 592 $cm^{-1}$ can be also attributed to the CuO stretching vibration. This is in good agreement with those IR active phonon modes calculated for CuO (530 and 590 $cm^{-1}$) [45, 46] and with experimental results obtained by Kliche and Popovic [40] (533 and 587 $cm^{-1}$) and Narang et al. [41] (515 and 586 $cm^{-1}$) for bulk polycrystalline CuO. It is also apparent that the sharp band at 621 $cm^{-1}$ in this spectrum is clearly indicative of the presence of $Cu_2O$. Thus, the bands exibited by the porous alumina after a.c. treatment in neutral to alkaline Cu(II)–TEA solutions are attributed to a CuO, $Cu_2O$, and $Cu(OH)_2$ mixture.

The spectra of porous alumina after a.c. deposition of copper into the template pores from acidic Cu(II)–TEA solution (Fig. 1a) show only a weak peak for $Cu_2O$. This suggests that copper deposited into the porous alumina from acid solutions in the metallic phase, colouring the template in cherry, contains some quantities of $Cu_2O$. This is probably due to the oxidation of the surface of metallic copper nanoparticles in air during template storage and preparation.

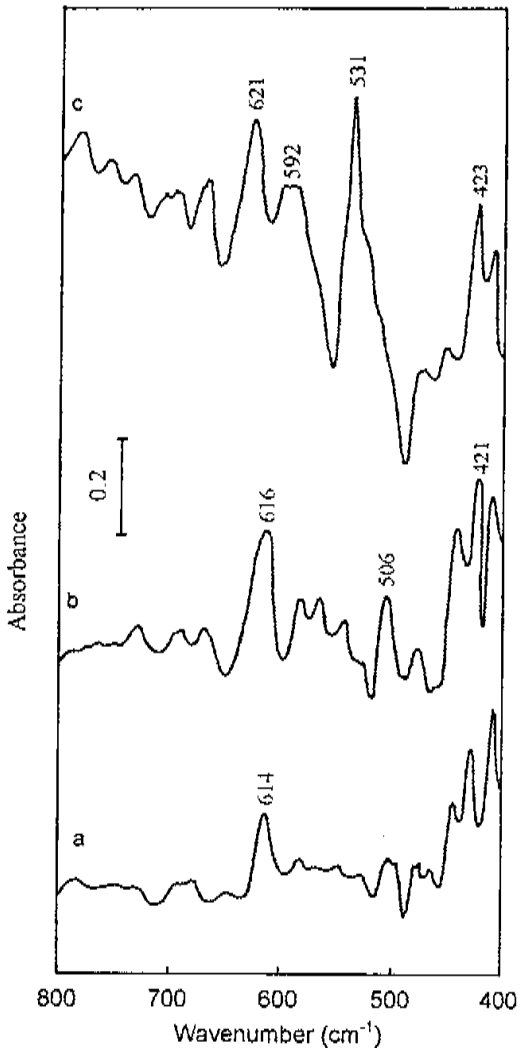


Fig. 1. Compensated FTIR spectra of porous alumina with copper oxygenous species deposited by a.c. electrolysis from 0.1 M $CuSO_4$ solution containing 0.05, 0.2, and 0.8 M TEA and $H_2SO_4$ up to pH: (*a*) 1.5, (*b*) 4.5, (*c*) 8.5. Al 99.5 %, δ 10 μm, $U_v$ 12 V

To determine the conditions of the Cu, $Cu(OH)_2$, $Cu_2O$, and CuO formation in the alumina pores during a.c electrolysis, quantitative analysis of the distribution of the copper complex species in various Cu(II)–TEA solutions had to be carried out. This analysis was based on equations of material balance and equilibria of all the species existing in solution. As has been reported earlier [47–51], in the solutions under investigation, certain copper complexes with TEA are formed (Table). Their equilibrium concentrations can be calculated on the basis of the material balance law, if the cumulative stability constants $\beta_{ij}$ of all the Cu complexes and the protonated

Table. **Quantitative characteristics of equilibria in the Cu / Cu(II) triethanolamine system**

| N° | Equilibrium | Stability Constant | Logarithm of constant | Ref. |
|---|---|---|---|---|
| 1 | $TEA + H^+ \leftrightarrow (TEA)H^+$ | $\beta^H_{TEA}$ | 7.9 | [47] |
| 2 | $Cu^{2+} + TEA + OH^- \leftrightarrow CuTEA(OH)^+$ | $\beta_{11}$ | 12.0 | [48, 50] |
| 3 | $Cu^{2+} + 2TEA \leftrightarrow Cu(TEA)_2^{2+}$ | $\beta_{20}$ | 6.68 | [49] |
| 4 | $Cu^{2+} + TEA + 2OH^- \leftrightarrow CuTEA(OH)_2$ | $\beta_{12}$ | 19.0 | [48, 50] |
| 5 | $Cu^{2+} + 2TEA + 2OH^- \leftrightarrow Cu(TEA)_2(OH)_2$ | $\beta_{22}$ | 19.0 | [48, 50] |
| 6 | $Cu^{2+} + TEA + 3OH^- \leftrightarrow CuTEA(OH)_3^-$ | $\beta_{13}$ | 21.0 | [48, 50] |
| 7 | $Cu^o + Cu^{2+} \leftrightarrow 2Cu^+$ | $\beta_{Cu(I)}$ | –6.22 | [51] |
| 8 | $Cu^{2+} + 2OH^- \leftrightarrow CuO_{(s)} + H_2O$ | $\beta_{Cu(II)s}$ | 20.1 | [30] |
| 9 | $2Cu^+ + 2OH^- \leftrightarrow Cu_2O_{(s)} + H_2O$ | $\beta_{Cu(I)s}$ | 29.7 | [30] |

species of TEA are known. The constants used in our calculations were taken from the works with similar Cu(II)–TEA solutions and are listed in Table. The material balance law for copper salt concentration ($c_{Me}$) in the solution yields

$$c_{Me} = [Cu^{2+}] (1 + \beta_{11}[TEA] [OH^-] + \beta_{20}[TEA]^2 + + \beta_{12}[TEA] [OH^-]^2 + \beta_{22}[TEA]^2[OH^-]^2 + \beta_{13}[TEA] [OH^-]^3). \quad (1)$$

The ligand equilibrium concentration is given by

$$c_{TEA} = [Cu^{2+}] \{\beta_{11}[TEA] [OH^-] + \beta_{20}[TEA]^2 + + \beta_{12}[TEA] [OH^-]^2 + \beta_{22}[TEA]^2 [OH^-]^2 + + \beta_{13}[TEA] [OH^-]^3\} + [TEA] (1 + \beta^H_{TEA}[H^+]). \quad (2)$$

Calculations by Eqs. (1) and (2), performed according to the method of Lewenberg-Marquardt interation [52], make it possible to determine equilibrium concentrations of $Cu^{2+}$ ions and TEA and the concentrations of all the complex species for each pH value. Calculated variations of $[Cu(TEA)_i(OH)_j]^{2-j}$ with pH for the typical solutions used for the a.c. deposition of copper and copper oxygenated compounds in the alumina pores are presented in Fig. 2. The data obtained at $c_{TEA}$ = 0.05 M show that the solutions of the ligand-deficient system are stable only at pH < 5.3 (Fig. 2a). An increase in pH causes precipitation of $Cu(OH)_2$, because reaction No 8 (Table) determines the critical (maximum) concentration of $Cu^{2+}$ ions, excess of which leads to the formation of bulk phase $Cu(OH)_2$. The pH range (highlighted by da.dotted lines in Fig. 2) specifies an unstable solution composition. This range becomes narrower with increasing $c_{TEA}$. However, in spite of $c_{TEA}$, there is always a certain pH range in which both copper aqua-complexes and insoluble solid species exist together. As has been previously reported [53, 54], the processes related to copper deposition and hydrogen evolution take place at the bottom of the alumina pores during a.c. electrolysis. As a result of hydrogen evolution (this fact will be

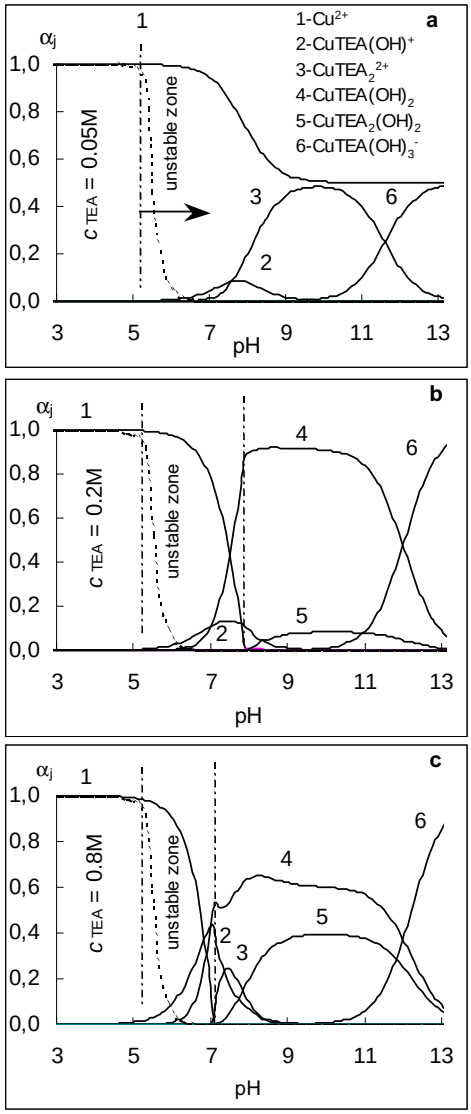


Fig. 2. Variations of concentration expressed by a molar fraction $\alpha_j$ equal to $[Cu(TEA)_i OH_j]/c_M$ of copper–containing species indicated by No 1,2,3… in part (*a*) with pH of the 0.1 M CuSO solution containing TEA (M): (*a*) 0.05, (*b*) 0.2, (*c*) 0.8. The da.dotted lines designate the pH values of the thermodynamically unstable composition of these solutions and dashed ones account for the formation of $Cu_2O$

explained later in more detail), the pH of the solution inside the alumina pores ought to increase [55, 56] and $Cu^+$ could be formed. In this case, all equations shown in Table are valid and will influence the equilibria concentrations of all copper species that exist in the solution. This should lead to changes in the solution composition until a universal equilibrium takes place again. Although, to our knowledge, there are no data relating to the existence of $Cu^+$ complexes with TEA, it is clear that the presence of insoluble copper compounds and appearance of $Cu^+$ ions in the solutions could cause some complications in the calculations of equilibrium concentrations of all species. Consequently, for the calculations of equilibrium $[Cu^+]$ formed in solutions at various pH, according to the reaction No 9 (non-thermodynamic in Table), the activity coefficients for $Cu^+$ and $Cu^{2+}$ ions must be known. In this circumstance, it is convenient to use an equation known as a Dawies expression, which is valid when the ionic strength (μ) of the solution is equal to 1.0 [57]

$$\log(\gamma_{(I)}) = -0.5\, z^2\, \mu^{0.5}\, (1-\mu^{0.5})^{-1} - 0.2\,\mu, \qquad (3)$$

where $\gamma_{(I)}$ and $z$ symbols denote the activity coefficient and charge of the $Cu^+$ ions, respectively. Hence, the concentration of $Cu^+$ ions obeys the equation

$$[Cu^+] = \gamma_{(II)}^{0.5}\, \gamma_{(I)}^{-1}\, [Cu^{2+}]^{0.5}\, \beta_{Cu}^{-0.5}, \qquad (4)$$

where $\gamma_{(II)}$ is the activity coefficient of $Cu^{2+}$ ions.

The ionic strength of the Cu(II)-TEA solutions under investigation decreases from about 0.9 at pH 3.0 to 0.2 at pH 10.5 (Fig. 3) due to an increase in the amounts of neutral Cu(II) species represented by curves 4 and 5 in Fig. 2. Variations of equilibrium $[Cu^+]$ and $[Cu^{2+}]$ with pH are calculated by solving Eqs. 1 and 2 and considering the influence of reactions Nos. 7–9 (Table) are shown in Fig. 4. As can be seen in Fig. 4, the deposition of copper only in metallic form from all acidic solutions with pH < 3 is most probable, since $[Cu^+]$ is limited only by reaction No 7 (curves 2 in Fig. 4). It is also worth mentioning that the formation of the bulk phase of $Cu_2O$ is impossible until the concentration of $Cu^+$ ions does not exceed the $[Cu^+]_{max}$ values. Based on the calculated variations of $[Cu^+]_{max}$ with pH of such solutions (curves 4), one can suggest that an imperceptible quantity of $Cu_2O$ equal to the difference between the equilibrium $[Cu^+]$ and $[Cu^+]_{max}$ could be formed, if the pH of acid Cu(II)–TEA solutions in the reaction zone increases due to hydrogen evolution so that reaction No 9 begins to control $[Cu^+]_{max}$. The results obtained also imply that in weakly acidic Cu(II)-TEA solutions (5 > pH > > 3) the production of $Cu_2O$ is most plausible,

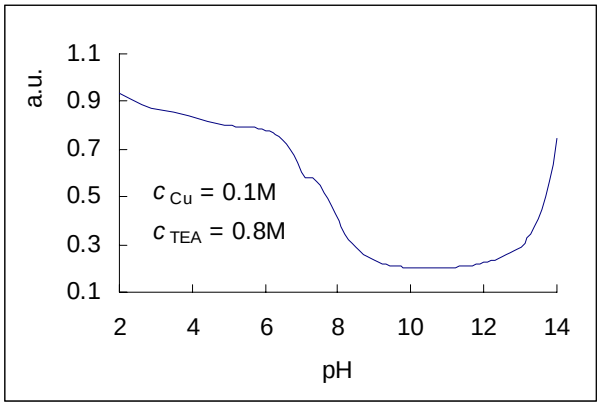


Fig. 3. Variation of the ionic strength μ with Cu(II)–TEA solution pH

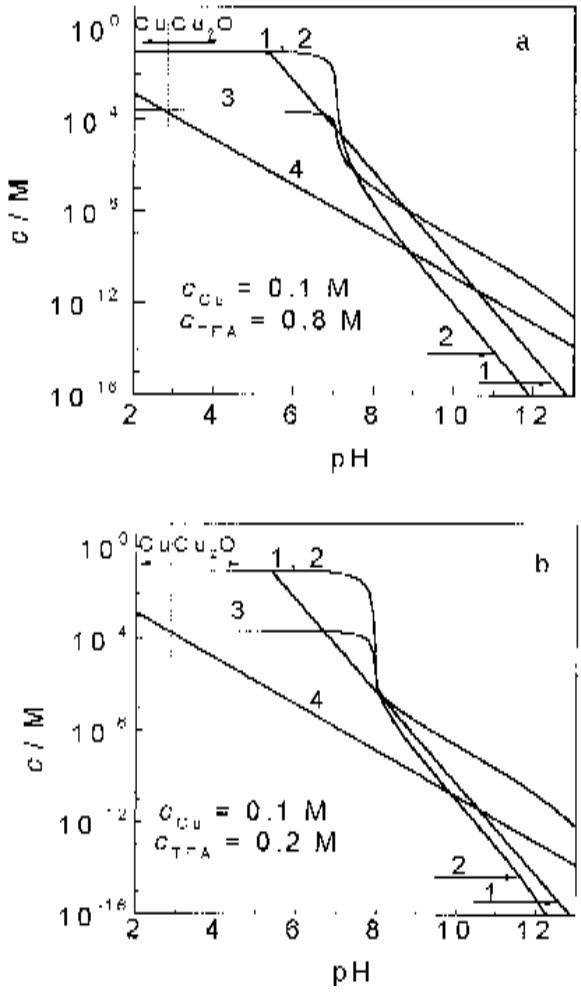


Fig. 4. Variation of equilibria concentrations of $Cu^{2+}$ (1, 2) and $Cu^+$ (3, 4) ions with pH of the Cu(II)–TEA solutions calculated: (*1*) according to Eq. 8 in Table 1, (*2*) by solving the system of Eqs. 1 and 2, (*3*) with regard to Eq. 7, and (*4*) with regard to Eq. 9 in Table 1

because in this pH region the dissolution of metallic copper species must occur via the reaction

$$Cu^0 + Cu^{2+} = 2\ Cu^+ \quad (5)$$

with conversion of $Cu^+$ ions eventually to $Cu_2O$ according to the scheme:

$$Cu^+ \rightarrow CuOH \rightarrow Cu_2O_{(s)}. \quad (6)$$

It is quite obvious from curve 4 in Fig. 4 that the equilibrium No 9 in Table limits the critical (maximum) concentration of $Cu^+$ ions. An increase in pH of these solutions higher than 5.0 due to hydrogen evolution should lead to the formation of a $Cu_2O$ and CuO mixture. A similar situation may be expected in alkaline Cu(II)–TEA solutions, where the obvious decrease of the equilibrium concentration of $Cu^{2+}$ ions (curve 2) and consequently the concentration of $Cu^+$ ions ought to decrease the rate of $Cu_2O$ formation. On the other hand, the formation of CuO in this pH region would be impossible as the redistribution of copper complex species should proceed quite rapidly. As can be seen from curve 2, the stability of Cu complex species in this pH region is controlled by the $[Cu^{2+}]$, which is obviously lower than $[Cu^{2+}]_{max}$ (curve 1). However, if the redistribution of Cu complex species is insufficiently quick, the increase in pH due to hydrogen evolution at the bottom of alumina pores can result in a considerable rate of CuO precipitation according to reaction No 8 in Table.

To investigate the processes occurring at the anodized aluminium electrode during cathodic cycle of a.c. electrolysis in various Cu(II) solutions, a potentiodynamic *I vs E* technique was used. It has been determined that porous alumina templates are coloured with the same tints as in the case of a.c. electrolysis, if the potential ($E_k$) during the first sweep in cathodic direction reaches a value of about 2/3 $U_a$. This result is attained when the potential sweep rate ($v$) is at least 0.1 V·s$^{-1}$ and the thickness of alumina ($\delta$) exceeds 7.0 μm (Fig. 5). Voltammetric investigations of porous alumina in Cu(II)–TEA solutions showed that there are two cathodic current peaks on $i(E)$ curves in these cases. An increase in $v$ shifted both peak potentials to more negative values, yielding a direct relationship between $v$ and $I_p$ in log-log scale (Fig. 6). The deposition of copper and/or copper containing species at the bottom of the alumina pores begins at more negative potentials of the first current peak, which for potential sweep rate of $v$ 0.2 V s$^{-1}$ and alumina grown in $H_2SO_4$ solutions at $U_a$ 15 and 25 V is equal to –10.2 and –16.4 V *vs* SHE, respectively. The current, which during cathodic potential sweep usually starts to rise below –1.5 V and depending on $v$ has a peak at –9.5 to –10.5 V, can be attributed only to a $H_3O^+$ and/or $H_2O$ reduction process at the bottom of alumina pores or at the aluminium/oxide interface, implying that the hydrogen evolution process should happen first. The fact that hydrogen evolution is the first process with an increasing cathodic potential should result in an excess of $OH^-$ ions at the bottom of the alumina pores, defining the copper deposit phase composition towards copper hydroxide/oxides formation.

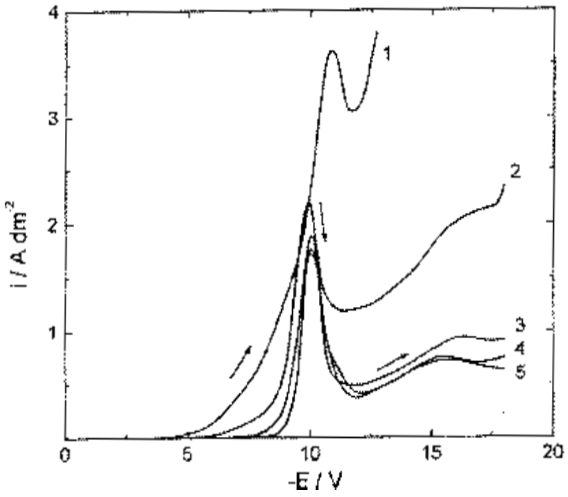


Fig. 5. Voltammograms of porous alumina grown in 1.53 M $H_2SO_4$ solution on 99.5% Al at 15 V up to the thickness $\delta$ (μm): 5 (*1*), 7 (*2*), 10 (*3*), 12.5 (*4*) recorded in the solution containing (M): $CuSO_4$ 0.1, TEA 0.8 and $H_2SO_4$ up to pH 8.5. $v$ = 0.2 V s$^{-1}$

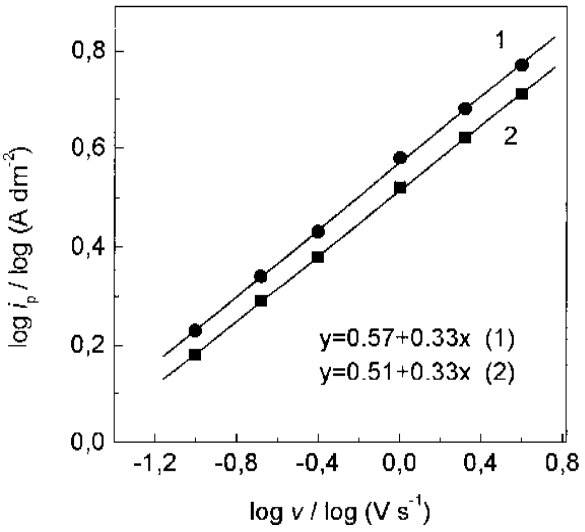


Fig. 6. Relationships between potential sweep rate $v$ and peak current of first wave in voltammograms of porous alumina as in Fig. 5 ($\delta$ 12 μm), recorded in a solution containing (M): $CuSO_4$ 0.1, $MgSO_4$ 0.1, and TEA up to pH 5.0 (1) and 8.0 (2)

## CONCLUSIONS

The IR spectrum of porous alumina after a.c. treatment in weakly acidic Cu(II)–TEA solutions was found to consist of the main peak located at 616 $cm^{-1}$ characteristic of $Cu_2O$ lattice vibrations and two at 421 and 506 $cm^{-1}$, characteristic of $Cu(OH)_2$. The species deposited into the alumina pores from alkaline solutions was found to be CuO (sharp and broad modes in FTIR spectrum at 531 and 592 $cm^{-1}$, respectively), $Cu(OH)_2$ and $Cu_2O$ mixture. The data were verified by calculations of equilibrium concentrations of all species in the solutions under investigation. The voltammetric studies showed that the first process, with the increasing cathodic potential, is $H_3O^+$ reduction resulting in an increase of pH in the bottom part of the alumina nanotubes up to the $Cu(OH)_2$ formation. A possible mechanism of the formation of copper oxygenous compounds during a.c. treatment in various Cu(II)-TEA solutions is discussed.

Received 17 April 2002
Accepted 7 June 2002

**References**

1. A. E. Rakhshni, *Solid State Electron*., **29**, 7 (1986).
2. I. G. Casella and M. Gatta, *J. Electroanal. Chem*., **494**, 12 (2000).
3. A. M. Youssef and E. A. El-Sharkawy, *Colloids and Surfaces A:* Physicochemical and Engineering Aspects, **138**, 21 (1998).
4. M. Frietsch, F. Zudock, and J. Goschnick, M. Bruns, *Sensors and Actuators, B: Chemical*, **65**, 379 (2000).
5. H. Gerisher, *J. Electroanal. Chem*., **82**, 133 (1977).
6. W. Zhang, M. Avignon, and K. H. Bennemann, *Phys. Rev*., **B 42**, 10192 (1990).
7. C. L. Huang, R. E. Partch, and E. Matijevic, *J. Colloid. Interface Sci*., **170**, 275 (1995).
8. A. Galembeck and O. L. Alves, *Synth. Met.,*. **102**, 1238 (1999).
9. R. T. Clay and R. E. Cohen, *New J. Chem*., 745 (1998).
10. J. F. Xu, W. Ji, Z. Z. Shen, S. H. Tang, X. R. Ye, D. Z. Jia, and X. Q. Xin, *J. Solid State Chem*., **147**, 516 (1999).
11. M. A. Brookshier, C. C. Chusuci, and D. W. Goodman, *Langmuir*, **15**, 2043 (1999).
12. R. Vijaya Kumar, R. Elgamiel, Y. Diamant, A. Gedanken, and J. Norwig, *Langmuir*, **17**, 1406 (2001).
13. E. C. Heltemes, *Phys. Rev*. **141**, 803 (1966).
14. C. A. Melendres, G. A. Bowmaker, J. M. Leger, and B. Beden, *J. Electroanal. Chem*., **449**, 215 (1998).
15. G. Kliche and Z. V. Popovic, *Phys. Rev.* **B 42**, 10060 (1990).
16. S. H. Narang, V. B. Kartha, and N.D. Patel, *Physica*, **C 204**, 8 (1992).
17. J. C. Hamilton, J. C. Farmer, and R. J. Anderson, *J. Electrochem. Soc*. **133**, 739 (1986).
18. G. Niaura, *Electrochim. Acta*, **45**, 3507 (2000).
19. D. W. Shoesmith, S. Sunder, M. G. Bailey, G. J. Wallace, and F. W. Stanchel, *J. Electroanal. Chem.*, **143**, 153 (1988).
20. U. Collisi and H.-H. Strehblow, *J. Electroanal. Chem*., **284**, 385 (1990).
21. G. Seshadri, H.-C. Xu, and J. A. Kelber, *J. Electrochem. Soc*., **146**, 1762 (1999).
22. H.-C. Xu, G. Seshadri, and J. A. Kelber, *J. Electrochem Soc*., **147**, 558 (2000).
23. G. Seshadri, H.-C. Xu, and J. A. Kelber, *J. Electrochem. Soc*. **148**, B222 (2001).
24. R. Babic, M. Metikoš-Hukovič, and M. Loncar, *Electrochim Acta*„ **44**, 2413 (1999).
25. R. Babic, M. Metikoš-Hukovič, and A. Jukie, *J. Electrochem. Soc*., **148**, B146 (2001).
26. H.-H. Strenhblow and B. Titze, *Electrochim. Acta* **25**, 839 (1980).
27. U. Sandez, H.-H. Strenhblow, and J. K. Dohrmann, *J. Phys. Chem*., **85**, 447 (1981).
28. M. Seo, X. C. Jiang, and N. Sato, *Werkst. Korros*., **39**, 583 (1988).
29. A. Survila, S. Kanapeckaite, and A. Surviliene, *J. Electroanal. Chem*., **501**, 151 (2001).
30. M. Pourbaix, *Atlas of Electrochemical Equilibria In Aqueous Solutions.* Pergamon Press, New York (1966) pp. 384–398.
31. H. Masuda, F. Hasegwa, and S. Ono, *J. Electrochem. Soc*., **144**, L127 (1997).
32. E. C. Heltemes, *Phys. Rev*., **141,** 803 (1966).
33. C. A. Melendres, G. A. Bowmaker, J. M. Leger, and B. Beden, *J. Electroanal. Chem.*, **449,** 215 (1998).
34. D. H. Sullivan, W. C. Conner, and M. P. Harold, *Appl. Spectrosc*., **46,** 811 (1992).
35. M. O?Keeffe, *J. Chem. Phys.*, **39,** 1789 (1963).
36. G. W. Poling, *J. Electrochem. Soc*., **116**, 958 (1969).
37. D. Persson and C. Leygraf, *J. Electrochem. Soc*., **140**, 1256 (1993).
38. D. E. Tevault, R. L. Mowery, R. A. DeMarco, and R. R. Smardzewski, *J. Chem. Phys.*, **74**, 4342 (1981).
39. H. Hagemann, H. Bill, W. Sadowski, E. Walker, and M. Francois, *Solid State Commun.*, **73**, 447 (1990).
40. G. Kliche and Z. V. Popovic, *Phys. Rev.*, **B 42**, 10060 (1990).
41. S. H. Narang, V. B. Kartha, and N. D. Patel, *Physica*, **C 204**, 8 (1992).
42. J. C. Hamilton, J. C. Farmer, and R. J. Anderson, *J. Electrochem. Soc*., **133**, 739 (1986).
43. H. Y. H. Chan, C. G. Takoudis, and M. J. Weaver, *J. Phys Chem*., **B 103**, 357 (1999).
44. D. L. Rousseau, R. P. Bauman, and S. P. S. Porto, *J. Raman Spectrosc*., **10**, 253 (1981).
45. C. Carabatos and B. Prevot, *Phys. Status Solidi*, **B 44**, 701 (1971).
46. P. Y. Yu and Y. R. Shen, *Phys. Rev*., **B 12**, 1377 (1975).

47. P. E. Sturrock, *Anal. Chem*., **35**, 1092 (1963).
48. A. Vashkelis, G. Klimantavichute, and A., Steponavichus, *Chemija B*, **3(80)**, 91 (1975).
49. V. Berdnikov and A. Purmal, *Zh. Fiz. Khim. USSR*, **56**, 1194 (1982).
50. L. G. Sillen and A. E. Martel (Eds), *Stability Constants of Metal-Ion Complexes*. Special Publications N° 17 and 25. Chemical Society, London **1**(1964); **2**(1971).
51. G. W. Tindall and S. Bruckenstein, *Anal. Chem*., **40**, 1402 (1968).
52. E. Polak, *Optimization Algorithms and Consistent Approximations*, N. Y., Springer Verlay (1997).
53. A. Jagminas and J. Giedraitiene, *Elektrokhimiyja*, **36**, 413 (2000).
54. V. Skominas, S. Lichušina, P. Miečinskas, and A. Jagminas, *Trans*. *IMF*, **79**, 213 (2001).
55. A. Jagminas and J. Giedraitienė, *Chemija (Vilnius)*, **11**, 55 (2000).
56. Y. Ishikawa and Y. Matsumoto, *Electrochim. Acta*, **46**, 2819 (2001).
57. C. W. Dawies, *Ion Association*. Butterworths, London (1962).

**A. Jagminas, V. Kapočius, O. Nivinskienė, S. Lichušina**

**VARIO IR VARIO DEGUONINIŲ JUNGINIŲ NUSODINIMO KINTAMĄJA SROVE IŠ CU(II)-TRIETANOLAMININIŲ TIRPALŲ Į ALUMINA AKUTES TEORINIAI ASPEKTAI**

S a n t r a u k a

FTIR tyrimais parodyta, kad silpnai rūgščiuose Cu(II)-TEA tirpaluose kintamosios srovės elektrolizės metu į aliuminio anodinio oksido (alumina) akutes nusodinamas $Cu_2O$ ir $Cu(OH)_2$ mišinys. Šarminiuose Cu(II)-TEA tirpaluose, turinčiuose daugiau ligando, į alumina akutes nusodinamas CuO su $Cu(OH)_2$ ir $Cu_2O$ priemaišomis. Nustatyti vario ir jo deguoninių junginių nusodinimo įvairaus rūgštingumo tirpaluose dėsningumai patvirtinti $Cu^{2+}$ ir $Cu^{+}$ turinčių dalelių termodinaminių pusiausvyrų skaičiavimais. Voltamperometriniais tyrimais parodyta, kad katodinio potencialo skleidimo sąlygomis ant akyto alumina elektrodo iš pradžių skiriasi tik vandenilis. Varis ir/ar jo deguoniniai junginiai alumina akutėse nusėda tik pasiekę vandenilio skyrimosi ribinės srovės potencialą, kai pH padidėjimas reakcijos zonoje ir jo dėka – netirpių Cu deguoninių junginių susidarymas yra visiškai tikėtini.